

Incorporation of tumor-targeting peptides into recombinant Adeno-associated virus capsids

Mirta Grifman, Martin Trepel, Paul Speece, Luz Beatriz Gilbert, Wadih Arap, Renata Pasqualini, Matthew D. Weitzman

Angaben zur Veröffentlichung / Publication details:

Grifman, Mirta, Martin Trepel, Paul Speece, Luz Beatriz Gilbert, Wadih Arap, Renata Pasqualini, and Matthew D. Weitzman. 2001. "Incorporation of tumor-targeting peptides into recombinant Adeno-associated virus capsids." *Molecular Therapy* 3 (6): 964–75.
<https://doi.org/10.1006/mthe.2001.0345>.

Incorporation of Tumor-Targeting Peptides into Recombinant Adeno-associated Virus Capsids

Mirta Grifman,^{*} Martin Trepel,^{†,1} Paul Speece,^{*,‡} Luz Beatriz Gilbert,^{*} Wadih Arap,[†] Renata Pasqualini,[†] and Matthew D. Weitzman^{*,2}

^{*}Laboratory of Genetics, The Salk Institute for Biological Studies, La Jolla, California 92186

[†]Department of GU Medical Oncology, University of Texas M. D. Anderson Center, Houston, Texas 77030

[‡]School of Medicine, University of California at San Diego, La Jolla, California 92093

Received for publication February 20, 2001; accepted in revised form May 7, 2001

The human parvovirus adeno-associated virus type 2 (AAV-2) possesses many features that make it an attractive vector for gene delivery *in vivo*. However, its broad host range may limit its usefulness and effectivity in several gene therapy applications in which transgene expression needs to be limited to a specific organ or cell type. In this study, we explored the possibility of directing recombinant AAV-2 transduction by incorporating targeting peptides previously isolated by *in vivo* phage display. Two putative loops within the AAV-2 capsid were examined as sites for incorporation of peptides. We tested the effects of deleting these loops and different strategies for the incorporation of several targeting peptides. The tumor-targeting sequence NGRAHA and a Myc epitope control were incorporated either as insertions or as replacements of the original capsid sequence. Viruses were assessed for packaging, accessibility of incorporated peptides, heparin binding, and transduction in a range of cell lines. Whereas recombinant viruses containing mutant capsid proteins were produced efficiently, transduction of several cell lines was significantly impaired for most modifications. However, certain mutants containing the peptide motif NGR, which binds CD13 (a receptor expressed in angiogenic vasculature and in many tumor cell lines), displayed an altered tropism toward cells expressing this receptor. Based on this work and previous studies, possible strategies for achieving *in vivo* targeting of recombinant AAV-2 are discussed.

INTRODUCTION

Adeno-associated virus type 2 (AAV-2) is a human parvovirus being developed into a promising delivery system for gene therapy applications. Recombinant adeno-associated virus (rAAV) vectors possess a number of attractive features, including lack of pathogenicity, ability to transduce both dividing and nondividing cells, and long-term transgene expression *in vitro* and *in vivo* (reviewed in 1, 2). rAAV vectors have been used to achieve expression of a large number of genes in a variety of cells and organs, including muscle, liver, brain, and lung (3–6). The wide host range of AAV may prove to be disadvantageous for systemic gene therapy, since it will result in transduction and possibly integration of the recombinant genome in

unwanted cells and tissues. The ability to redirect rAAV infectivity and host range will circumvent these problems and may also enable the administration of lower doses of vector. Certain tissues and cell types are naturally resistant to rAAV transduction. These include human leukemia cell lines, airway epithelia, and CD34⁺ cells (7–11). This may be due to the absence of receptors for AAV or other intracellular factors involved in infection. Heparan sulfate proteoglycan has been reported to be the primary attachment receptor for AAV-2 (12). In addition, human fibroblast growth factor receptor 1 (FGFR-1) and $\alpha_v\beta_5$ integrin have been proposed to act as secondary receptors (13, 14). Following receptor binding, AAV-2 particles enter the cell via receptor-mediated endocytosis through clathrin-coated pits, and dynamin is also involved in AAV-2 trafficking through the cytoplasm via microfilaments and microtubules (15–17). Most of the virus particles accumulate in a perinuclear pattern, with a slow entry of intact virions into the nucleus (17–19).

AAV particles have a diameter of 20–25 nm and contain a single-stranded genome of approximately 4700 nucleotides (20–22). The genome contains two open reading

¹ Present address: Department of Hematology and Oncology, The University of Freiburg Medical Center, Freiburg, Germany.

² To whom correspondence and reprint requests should be addressed at the Laboratory of Genetics, Salk Institute for Biological Studies, P.O. Box 85800, San Diego, CA 92186-5800. Fax: (858) 558 7454. E-mail: weitzman@salk.edu.

frames, designated *rep* and *cap*, flanked by inverted terminal repeats which contain all the *cis* requirements for replication and packaging (23). Using alternate splicing and different translational initiation codons the virus generates three structural proteins, VP1, VP2, and VP3, from the *cap* gene (24). The small icosahedral capsid is composed of 60 subunits with a relative stoichiometry of 1:1:10 for VP1, VP2, and VP3. Although the three-dimensional structure of the AAV capsid has not yet been determined, those of some related parvoviruses have been solved by X-ray crystallography. The atomic structures are known for canine parvovirus (CPV) (25), feline panleukopenia virus (26), minute virus of mice (27), and the human parvovirus B19 (28). Parvoviral capsids contain a core structure comprising an eight-stranded β -barrel motif, similar to other icosahedral viruses. Between several strands of the β -barrel are large insertions that make up the majority of the capsid's surfaces. The surface features of the CPV capsid include a hollow cylinder at the fivefold axis of symmetry which is surrounded by a circular depression (canyon), a prominent protrusion at the threefold axis of symmetry (threefold spike), and a depression (dimple), spanning the twofold axis of symmetry. Alignments of parvoviral capsids reveal a high sequence conservation in the strands which make up the β -barrel motif (29). In contrast, sequence homologies in regions that code for the surface of the capsid are lower, consistent with an involvement in determining the different viral host ranges. Despite a divergence in sequence, antigenic sites are often located in analogous regions. Recently, several antigenic regions of AAV-2 have been mapped (30, 31) and their involvement in AAV-2-cell interaction and neutralization of AAV-2 infection was studied. Based on sequence alignments, most antigenic peptides in AAV correspond to similarly exposed regions in the different parvoviruses and they putatively map to the cylinder, the threefold spike loop, and the region between the twofold depression and the threefold spike (30, 31).

Strategies currently being explored for targeting viral vectors include bispecific conjugates and genetically modified capsids. Both of these approaches have recently been adapted for rAAV vectors (reviewed in 31a). In one study bispecific antibodies recognizing the AAV-2 viral capsid and a specific cell surface receptor were employed to re-target AAV-2 to human megakaryocytes that were non-permissive for normal AAV infection (9). The use of bispecific conjugates is not always amenable to scale-up for clinical production and they also suffer from instability *in vivo*. Therefore a more attractive approach to vector retargeting is the genetic incorporation of targeting peptides into the rAAV capsid. The first attempt at expanding the tropism of AAV fused the single-chain variable fragment of a monoclonal antibody against human CD34 protein onto the N-terminus of the VP2 capsid protein and demonstrated improved infectivity of hematopoietic progenitor cells (32). Several recent reports have begun to address structural features of AAV capsids in order to identify sites amenable to incorporation of peptides. One study suggested six possible sites in the AAV capsid that were pre-

dicted to be within surface loops (33). A 14-amino-acid targeting peptide (L14) containing an RGD sequence was inserted into these sites and virus was produced. In three mutants the peptide was exposed on the capsid surface and one of these showed preferential transduction of integrin-expressing cells. Rabinowitz *et al.* employed linker insertional mutagenesis to place small peptide sequences (three to five amino acids) randomly across the entire capsid coding region (34). Mutants fell into three phenotypic groups, depending on their ability to assemble capsids, package DNA, and transduce cells. Recently, Wu *et al.* reported a broad mutational analysis of the AAV-2 capsid that identified several sites amenable to the incorporation of peptides (35). They also identified regions involved in heparin binding and were able to demonstrate altered tropism of viruses engineered to contain the serpin receptor ligand. It has been shown that the accessibility of incorporated peptides can also be affected by the composition of flanking residues (J. Bartlett, personal communication).

A combination of two important parameters will determine the success of genetically modified capsids for retargeting viral vectors *in vivo*. The first decision is to choose the location for insertions. The site must be such that (i) assembly and packaging of the virus capsid are not affected and (ii) peptides must be exposed on the surface of the virus. The second parameter is the choice of targeting peptide. In order for a rAAV vector to be directed to a specific tissue following intravenous administration it will require (i) that its natural tropism be diminished and (ii) that it contains a ligand that will recognize a receptor accessible through the circulation and selectively expressed in the organ or tissue of interest. The versatility of phage display technology has made it possible to screen for targeting peptides *in vivo*. The screening process involves injecting a phage library into an experimental animal and rescuing phage from the desired target by infecting host bacteria with tissue extract. Repeated selection yields phage that home preferentially to the target tissue (36, 37). Thus far, this method has been used to explore the vascular specificity of various peptides after their intravenous injection into mice and rats. Peptides capable of homing to the vasculature of organs and tumor tissues have been identified in this manner, attesting to the power of the method (36–38). Peptides targeting selective markers in the vasculature of specific organs or tissues are therefore attractive for incorporation into recombinant viral vectors for targeted gene delivery.

In this study we have explored genetic modification of the AAV-2 capsid by introducing a peptide motif, NGR, which targets a receptor, CD13 (39), that is specifically upregulated in angiogenic vasculature. CD13 is a key regulator of angiogenesis and functions as a vascular receptor for the NGR motif in activated blood vessels (39). The NGR motif has been successfully employed to enhance the antitumor properties of doxorubicin and tumor necrosis factor (TNF) (38, 40). Based on sequence homologies and on the results of previous studies, we chose two sites corresponding to CPV loops 3 and 4 (25). We eval-

uated the impact of deletions, replacements, and insertions within these loops. We inserted sequences coding for the motif NGR (38, 39), other organ-homing peptides (36, 37, 41), or a Myc epitope tag. Recombinant AAV vectors expressing reporter genes were generated with modified Cap proteins and analyzed for virus production, heparin binding, and transduction assays. We show by immunoprecipitation of epitope-tagged virions that these loops are presented on the surface of the capsid, although the degree of accessibility varied. Deletions, modifications, or insertions within the loops did not affect virus production. Deletion and large insertions at one of the loops abolished heparin binding. Transduction of several cell lines was significantly impaired for most deletions, mutations, and insertions. However, several mutants containing the NGR peptide displayed an altered tropism toward cells expressing CD13. These results are discussed in light of recently reported data, to suggest strategies for the incorporation of targeting peptides for systemic gene therapy.

MATERIALS AND METHODS

Plasmids. Plasmid pXX2 (42) was used as a template for the construction of all modified capsids. Plasmids with deletions of the loop regions (pXX2- Δ LoopIII and Δ LoopIV) were generated by elongation PCR, introducing novel *MluI* and *SpeI* sites as shown in Fig. 2. The restriction sites were designed to allow for the in-frame insertion of oligonucleotides coding for foreign epitopes. All replacements and insertions were generated from these plasmids, except for insertions at the 588 site, which were cloned using a novel *SpeI* site introduced at nucleotide 3967 of AAV2 (GenBank Accession No. AF043303). All mutated plasmids were sequenced using an automated ABI Prism DNA sequencer 377 (PE Biosystems, Foster City, CA). Plasmid pXX6 supplies the adenovirus helper proteins for rAAV production (43) and pAAV-GFP contains a recombinant AAV genome with the green fluorescent protein flanked by viral inverted terminal repeats and expressed from a cytomegalovirus promoter.

Cell culture, transfection, and virus production. All cell lines were maintained in Dulbecco's modified Eagle's medium supplemented with 10% fetal bovine serum (FBS). Transfections were performed by calcium phosphate precipitation according to standard protocols and repeated multiple times. To produce rAAV with mutant capsid proteins, we transfected 293T cells with three plasmids: pXX2, which supplied wild-type or mutant capsid proteins; pXX6, which contained the adenovirus helper functions; and pAAV-GFP. For virus production 5×15 -cm plates were transfected each with 6 μ g pXX2, 25 μ g pXX6, and 19 μ g pAAV-GFP and incubated at 37°C for 72 h. Virus was purified using iodixanol gradients as described elsewhere (44). Wild-type adenovirus type 5 (Ad5) used for titration of transduction was propagated in 293 cells and purified by sequential rounds of ultracentrifugation in CsCl gradients. Titers of Ad5 were determined by plaque assay on 293 cells.

Virus titers, transduction assays, and FACS analysis. The titer of rAAV genome-containing particles per milliliter was determined by real-time PCR using SYBR Green I double-stranded DNA binding dye and an ABI Prism 7700 Sequence Detection System (PE Biosystems). Samples were prepared as previously described (45). The following primers were chosen to amplify eGFP: F1, CTGCTGCCCCACAACCA, and R2, CCATGTGATCGCGCTTCTC).

To assess transduction, cells grown in 24-well dishes were infected with rAAV (100–10,000 genomes/cell) and Ad5 (5 plaque forming units/cell) in fresh medium with 10% FBS. Ad5 co-infection was used to maximize transduction by rAAV by enhancement of second-strand synthesis as previously reported (54). Transduction by rAAV-GFP was determined by counting green cells using an Axiovert25 microscope (Carl Zeiss, Thornwood, NY) equipped with an OSRAM HBO mercury short arc lamp microscope or by FACS analysis using a Becton–Dickinson FACScan (San Jose,

CA) with a 488-nm laser excitation. Transduction was measured 24–48 h following infection. Cells were photographed using a Nikon (Garden City, NY) microscope in conjunction with a charge-coupled device camera (Cooke Sensicam; Cooke Corp., Tonawanda, NY) and images were captured using SlideBook (Intelligent Imaging Innovation, Denver, CO). All transduction experiments were repeated at least three times. Expression of CD13 was measured by FACS using the antibody WM15 (Pharmingen, San Diego, CA). Each cell type was gated based on the fluorescence obtained when incubated with mouse IgG antibody. Mouse anti- β 1 integrin, clone P4C10 (Life Technologies, Rockville, MD), was used as a positive control (100% gated).

Gel electrophoresis, Western blotting, immunoprecipitations, and heparin binding assays. An equal number of purified rAAV-GFP virions (10^9 genome-containing particles) were separated on 8% SDS-polyacrylamide gels and Western blotting was performed to detect capsid proteins. In all cases proteins were detected by enhanced chemiluminescence (NEN, Boston, MA, and Amersham, Buckinghamshire, UK) according to the manufacturer's instructions. AAV capsid proteins were detected with mAb B1 (American Research Products (ARP), Belmont, MA). Immunoprecipitations were performed from iodixanol-purified rAAV. Equivalent amounts of purified virus (10^{10} genome-containing particles) were precleared with protein G–Sepharose (Amersham/Pharmacia, Piscataway, NJ) for 1 h at 4°C in RIPA buffer (20 mM Tris, pH 8.0, 100 mM NaCl, 0.2% NP-40, 0.2% Triton X-100, and 0.2% deoxycholate). Samples were centrifuged and the supernatants containing the rAAV particles were incubated at 4°C overnight with antibodies A20 (ARP), A69 (ARP), or anti-Myc (Invitrogen, Carlsbad, CA) or a control antibody. Samples were washed four times in RIPA buffer. After being washed, pellets were boiled for 5 min in SDS-PAGE loading buffer. Proteins were separated on 8% SDS-polyacrylamide gels and capsid proteins detected by Western blotting with the B1 antibody.

Viruses with wild-type virions and deletions, insertions, or replacements (10^{10} genome-containing particles) were bound to 100 μ l heparin agarose (Sigma, St. Louis, MO) in binding/washing buffer (20 mM Tris, pH 7.6, 150 mM NaCl, and 1 mM $MgCl_2$) for 1 h at 4°C. After six washes, bound virus was eluted with elution buffer (20 mM Tris, pH 7.6, 1 M NaCl). The fractions were detected by Western blotting using the B1 antibody.

RESULTS

Alignments of Parvovirus Cap Proteins

In order to identify suitable sites for insertion of targeting peptides, we aligned the amino acid sequences of several parvoviruses. We performed sequence alignments using the MacVector software package (Oxford Molecular Group, UK) and included recently reported sequences for AAV serotypes 1, 3, 5, and 6 (46–50). Antigenic sequences of AAV-2 are aligned to the corresponding regions of CPV in Fig. 1 and are shown as four domains, I, II, III, and IV, which contain loops 1–4 of CPV (25). We have marked on these alignments peptides previously identified as antigenic sites (see boxes 1–14).

An antigenic region in domain I of CPV (box 3) is the target of neutralizing antibodies (51, 52). Interestingly, a nonconserved amino acid sequence of B19, which is also the target for neutralizing antibodies (box 2) maps to the same site (53). A peptide containing sequences of AAV-2 which partially overlap with loop 1 of CPV based on sequence alignments has been shown to inhibit the binding of neutralizing antibodies to AAV in an ELISA (31). A minor component of the epitope recognized by the monoclonal antibody A20 (box 4) also aligns within this region (30), but this antibody does not inhibit cell binding. Mutations in either of these two epitopes have been

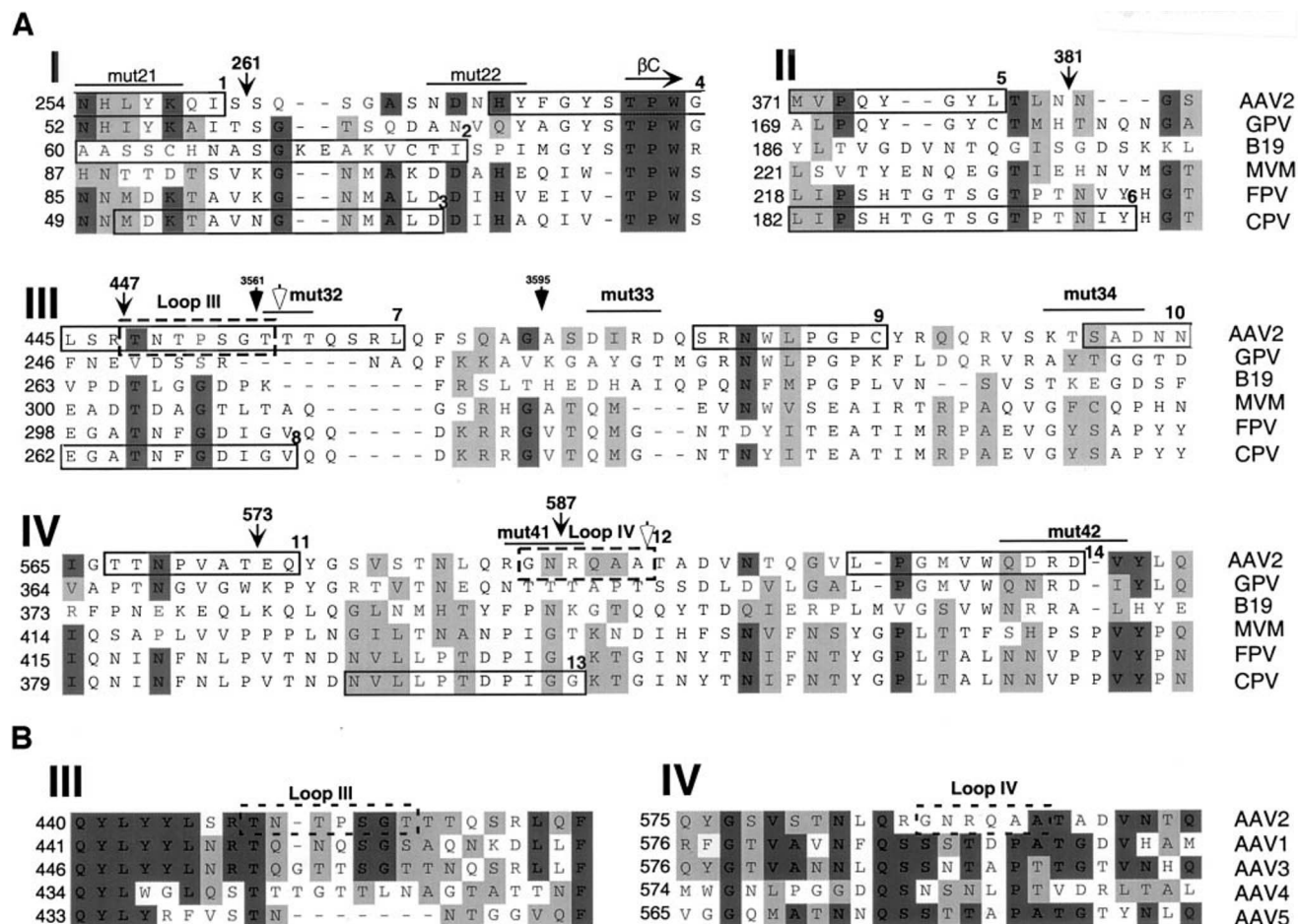


FIG. 1. Homology alignments of parvovirus Cap proteins. (A) The amino acid sequences of the capsid proteins of AAV-2, Genpept Accession No. (GP No.) 2906023; goose parvovirus (GPV), 9628653; B19, GP No. 4092542; minute virus of mice (MVM), GP No. 2982110; feline panleukopenia virus (FPV), GP No. 494031; and canine parvovirus (CPV), GP No. 494746, were aligned using the ClustalW alignment tool of the software program MacVector (Oxford Molecular Group, London). The alignments are shown for four domains (I–IV) within the capsid protein, which contain the antigenic loops of CPV. Identical sequences (dark blue) and similar sequences (light blue) are highlighted. Antigenic regions within the loops are enclosed by boxes that are numbered to the right (see text for details and references). Published mutations and their corresponding sites are indicated and part of the β -barrel is shown with a horizontal arrow. Sites of insertions are marked with an arrow (33), filled arrowhead (34), and open arrowhead (35). Numbering of mutations and sites match the corresponding papers. (B) Alignments of putative Loops III and IV of the AAV serotypes. The sequences of AAV serotypes 2, 1, 3, 4, and 5 are aligned, and regions modified in this study are shown enclosed by dashed boxes.

shown to severely impair transduction or destabilize the AAV capsid (35). A second major antigenic site of CPV lies within domain II (box 6) (25). An AAV-2 peptide (box 5) sequence forms an epitope, in conjunction with the peptide A-20 in domain I (box 4), that is recognized by a monoclonal neutralizing antibody. Taken together, these results imply that domains I and II are in close proximity in AAV-2. Moreover, the inability of the antibody that recognizes this region to inhibit receptor binding suggests that this region in AAV-2 is not involved in receptor recognition, but may have an important function in a later event in the infectious pathway. These putative loop regions are also well conserved between the different AAV serotypes (50). Therefore, it seems unlikely that insertion of targeting peptides at these loops would lead to targeted AAV transduction.

Several residues in antigenic loop 3 of CPV and the

corresponding residues in related parvoviruses have been shown to be involved in viral tropism. One of the major neutralizing epitopes in CPV (box 8) is in the extended portion of loop 3 on the shoulder of the threefold spike (51). The AAV-2 sequence that aligns to this region (box 11) is also able to bind neutralizing antibodies; however, its involvement in receptor attachment is still not clear (31). All AAVs except serotype 5 contain an insertion at this site compared to other parvoviruses (Figs. 1A and 1B). Two monoclonal antibodies against AAV-2 recognize additional epitopes within domain III (boxes 9 and 10). Moreover, two charge-to-alanine mutations in this region resulted in the production of viruses defective in transduction (35). Rabinowitz *et al.* found that small insertions in this region also resulted in decreased transduction (34). However, insertion of the L14 peptide at residue 447 of the AAV-2 capsid protein resulted in exposure on the

surface of the capsid and increased binding to cells expressing integrins, but this virus did not retarget transduction.

Domain IV of AAV-2 contains two sequences which have been mapped as targets of neutralizing antibodies (boxes 11 and 14). Mutations in one of these epitopes resulted in an inability to assemble capsids (35). Mutations and insertions have also shown the involvement of an adjacent site (box 12) in heparin binding. Although both regions are variable between AAV serotypes (50), Fig. 1B shows that domain IV is more conserved. Based on the sequence alignments and previous findings, we decided to analyze different strategies for the incorporation of organ-targeting peptides into putative loops within domains III and IV of AAV-2. We have designated these Loop III and Loop IV (dotted boxes 7 and 12).

Effects of Deletions within Putative Loops III and IV of AAV-2

We first asked whether predicted Loops III and IV were essential for virus assembly and packaging by making deletions within these regions. Mutant plasmids were generated to encode capsid proteins with deletions of 7 or 6 amino acids within Loop III and Loop IV, respectively (Fig. 2A). These constructs were transfected together with a vector plasmid (pAAV-GFP) and an adenovirus helper plasmid (pXX6) into 293 cells to generate the mutant viruses rAAV-GFP- Δ III and rAAV-GFP- Δ IV. Viruses were purified by iodixanol gradient ultracentrifugation and the amount of genome-containing particles was assessed by real-time PCR. The number of genome-containing particles for the viruses with the mutated Cap proteins was similar to that of those generated with wild-type Cap proteins (Fig. 2B). The protein composition of virions was determined by Western blotting of proteins from virus preparations having equivalent numbers of genome-containing virions. The stoichiometry of the three Cap proteins was similar to that of wild-type capsids. The ability of the viruses to transduce target cells was assessed by FACS analysis and fluorescence microscopy. As can be seen in Fig. 2C, transduction of 293 cells was significantly impaired for viruses with deletions in Loop III or IV, compared to virus generated with wild-type Cap proteins. These data suggest that the deleted portions of Loops III and IV are not essential for assembly or packaging of rAAV virions but that they have important roles in transduction.

Accessibility of Replacements or Insertions at Loops III and IV

Having shown that Loops III and IV were nonessential for assembly and packaging of AAV capsids we next assessed whether heterologous peptides inserted at these locations were presented on the surface of the virion. We first replaced the natural sequences of the loops with oligonucleotides encoding a Myc epitope. In addition to replacements of deleted sequences, we also selected two sites within Loops III and IV for insertion of targeting peptides. One of these sites was at amino acid 449 within

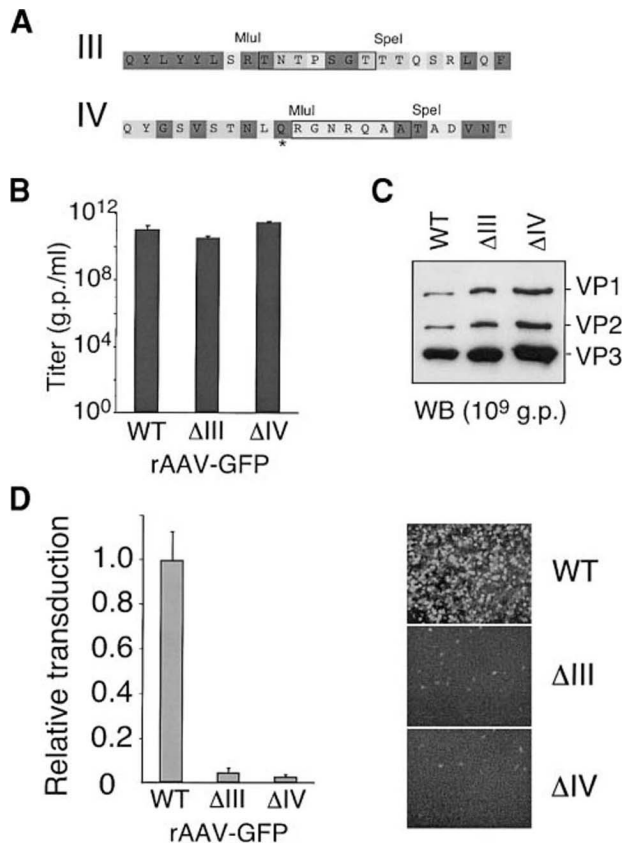


FIG. 2. Effects of deletions within putative Loops III and IV of AAV-2. (A) Constructs were generated with deletions in putative Loops III and IV. Sites of restriction enzymes *SpeI* and *MluI* used for cloning oligonucleotides are indicated. Sequences conserved between AAV serotypes are highlighted. Mutation of a single residue (Q), marked with an asterisk, prevented efficient transduction (see text for details). Enclosed boxes marked regions deleted. (B) Effect of deletions on number of genome-containing particles. Recombinant viruses with wild-type or mutant capsids were generated by transfections and purified by iodixanol gradients. Purified genome-containing rAAV vectors were quantified by real-time PCR against plasmid standards and are represented as genome-containing particles/ml (g.p./ml). (C) Virion composition of purified capsids. After iodixanol gradient purification an equal quantity of genome-containing virions as determined by real-time PCR (10⁹ genomes) was analyzed by Western blotting with antibody B1. The positions of the capsid proteins VP1, VP2, and VP3 are indicated. (D) Deletions in Loops III and IV of AAV Cap proteins impair rAAV transduction. Transduction of 293 cells infected with rAAV-GFP at an m.o.i. of 1000 genomes/cell in the presence of Ad5 (m.o.i. 5 pfu) was assessed after 24–48 h by analyzing GFP expression by FACS analysis (left) or fluorescence (right).

Loop III and the second was at amino acid 588, which is in predicted Loop IV. The positions of these sites imposed on the CPV structure crystal structure are shown in Fig. 3A. Loop III is present in an extended conformation protruding from the virus, while Loop IV is in a pocket conformation, consistent with its putative function as a receptor anchor. These sites are similar but not identical to those recently used by others (33, 35).

In order for these sites to be useful in retargeting AAV vectors, it is necessary for inserted peptides to be presented on the surface of the virion. To determine the relative accessibility of peptides at these sites, we assessed the ability of

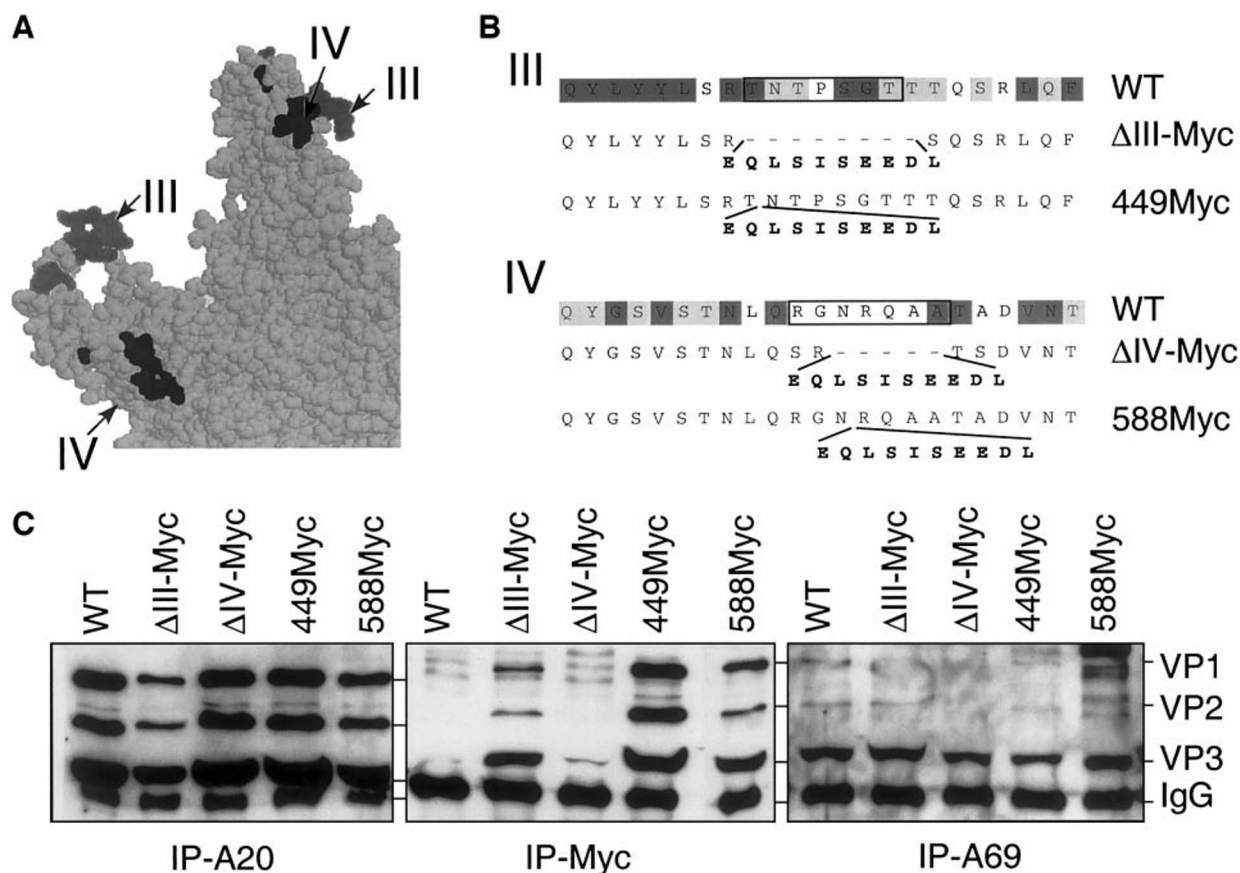


FIG. 3. Insertions or replacements in Loops III and IV are exposed on the capsid surface. (A) The positions of antigenic Loops III (green) and IV (blue) are shown as filled dots on the structure of the CPV Cap protein. (B) A peptide encoding the Myc epitope tag either replaced Loops III or IV or was inserted at residues 449 and 588. Sequences conserved between AAV serotypes are highlighted. (C) The accessibility of the Myc epitope in the fully assembled capsid was assessed by immunoprecipitation, followed by Western blotting. For each construct rAAV-GFP was generated by transfection and particles purified by iodixanol gradients. Similar numbers of genome-containing particles (10^{10}) were immunoprecipitated using antibodies that recognize intact AAV viral particles (A20), the Myc epitope, or VP2 capsid proteins (A69). Immunoprecipitated proteins were detected with an anti-Cap antibody (B1). The positions of VP1, VP2, and VP3 are indicated.

an anti-Myc antibody to immunoprecipitate epitope-tagged capsids (Fig. 3). Constructs for the mutant viruses were transfected into 293 cells together with the rAAV-GFP vector plasmid and the adenovirus helper plasmid. Cells were harvested and rAAV was purified by iodixanol gradients. The number of genome-containing particles was assessed by real-time PCR. Equal numbers of particles (10^{10} genome-containing particles) were immunoprecipitated using antibodies that recognize either intact AAV viral particles (A20) or the Myc epitope (Fig. 3C). Western blotting with an anti-Cap antibody (B1) demonstrated that the A20 antibody could isolate wild-type and mutant virions with equal efficiency. Control wild-type virus was not precipitated with the Myc antibody. In contrast, the Myc antibody was able to capture capsids containing the Myc epitope in Loops III and IV. The efficiency of capsid precipitation by the Myc antibody was higher for the insertions (rAAV-449Myc and rAAV-588Myc) compared to the loop replacements (rAAV-ΔIII-Myc or rAAV-ΔIV-Myc). We confirmed that the differences between viruses did not reflect immunoprecipitation of unassembled soluble proteins, by using an antibody to

VP2 that also recognizes nonassembled Cap proteins (A69). Using this antibody similar levels of Cap proteins were detected with all viruses. No virus Cap proteins were detected using an antibody against a cellular protein as a negative control (data not shown). These experiments demonstrated that in most cases the Myc epitope was accessible to the antibody and was therefore presented on the surface of the assembled virions. These data confirm the findings of Girod *et al.* and Wu *et al.* (33, 35), who demonstrated surface exposure of the L14 peptide and HA tag, respectively, when inserted at adjacent sites. These results also highlight possible differences in the exposure of epitopes when present as replacements compared to insertions.

Effects of Replacing or Inserting Targeting Peptides into Putative Loop III or IV of AAV-2

Having established that sequences could be mutated or inserted in the putative Loops III and IV, we sought to assess the effects of incorporating targeting peptides at these sites. The tripeptide asparagine-glycine-arginine

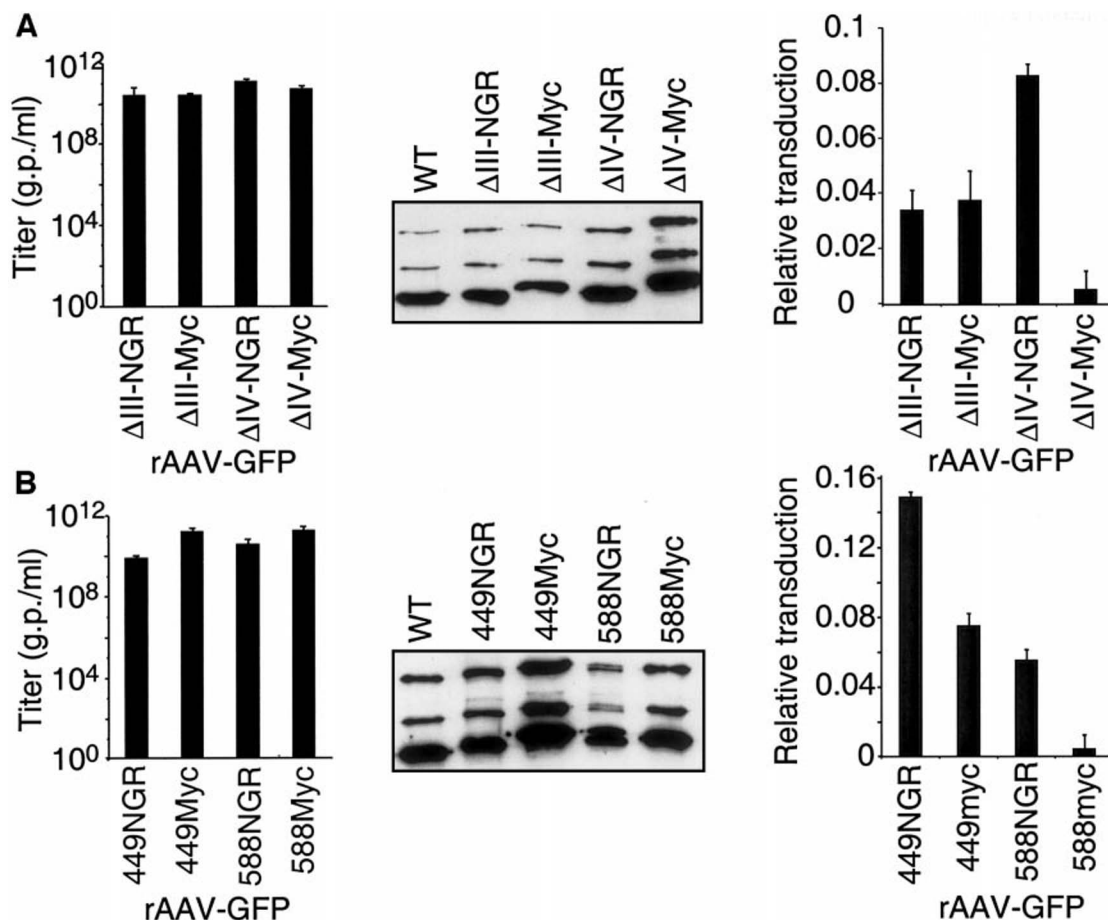


FIG. 4. Effects of replacements or insertions within the putative loops. Effects of loop replacements (A) or peptide insertions (B) on vector titers. Purified viruses were quantified by real-time PCR against plasmid standards and are represented as genome-containing particles/ml (g.p./ml) (left). Virion composition of wild-type and mutant viruses after iodixanol purification was assessed by Western blotting (center). Equal quantities of purified virions as determined by real-time PCR (10^9 genomes) were subjected to SDS-PAGE and Cap proteins detected by Western blotting with antibody B1. Replacements and insertions within regions of Loops III and IV of the AAV Cap impair rAAV transduction (right). Transduction of 293 cells infected with rAAV-GFP at an m.o.i. of 1000 in the presence of Ad5 (m.o.i. 5 pfu/cell) for 24–48 h was quantified by FACS analysis. Presented are transductions relative to wild-type capsids.

(NGR) was isolated using the *in vivo* phage selection system in which peptides capable of homing to tumor angiogenic vasculature were recovered from phage libraries. Peptides containing an NGR motif bind selectively to CD13 *in vivo* in tumor- and hypoxia-activated blood vessels (39). Oligonucleotides encoding this sequence were cloned into the putative loops, either as replacements of the original sequence or as insertions. Recombinant viruses for the replacements (rAAV-ΔIII-NGR or rAAV-ΔIV-NGR) or insertions (rAAV-449NGR and rAAV-588NGR) were generated by transfections and purified by iodixanol gradients. Control viruses contained the Myc epitope as a replacement (rAAV-ΔIII-Myc or rAAV-ΔIV-Myc) or insertion (rAAV-449Myc and rAAV-588Myc) at the same sites. The numbers of genome-containing particles were determined by real-time PCR and in all cases they were comparable to those obtained with wild-type capsid proteins (Fig. 4). The stoichiometry of these purified capsids was determined by Western blotting with a Cap antibody and remained the same with all modified capsids.

First, we tested the ability of the engineered viruses containing replacements or insertions to transduce 293T cells. Cells were transduced with 1000 genome-containing particles of rAAV per cell in the presence of adenovirus co-infection to maximize transduction (54). Despite their ability to assemble and package AAV particles, these mutant viruses were significantly impaired for transduction in 293T cells, with efficiencies ranging from 0.5 to 15% of wild-type (Fig. 4). Transduction was most severely impaired for viruses that contained the Myc epitope in Loop IV, either as a replacement or as an additional insertion. A titration of infections over a range of m.o.i. revealed that regardless of the amount of particles used, rAAV-ΔIV-Myc and rAAV-588Myc were unable to achieve more than 0.5% the transduction efficiency of wild-type virions (data not shown). These results confirm that targeting peptides can be inserted into the putative loops without affecting assembly and packaging but transduction is impaired.

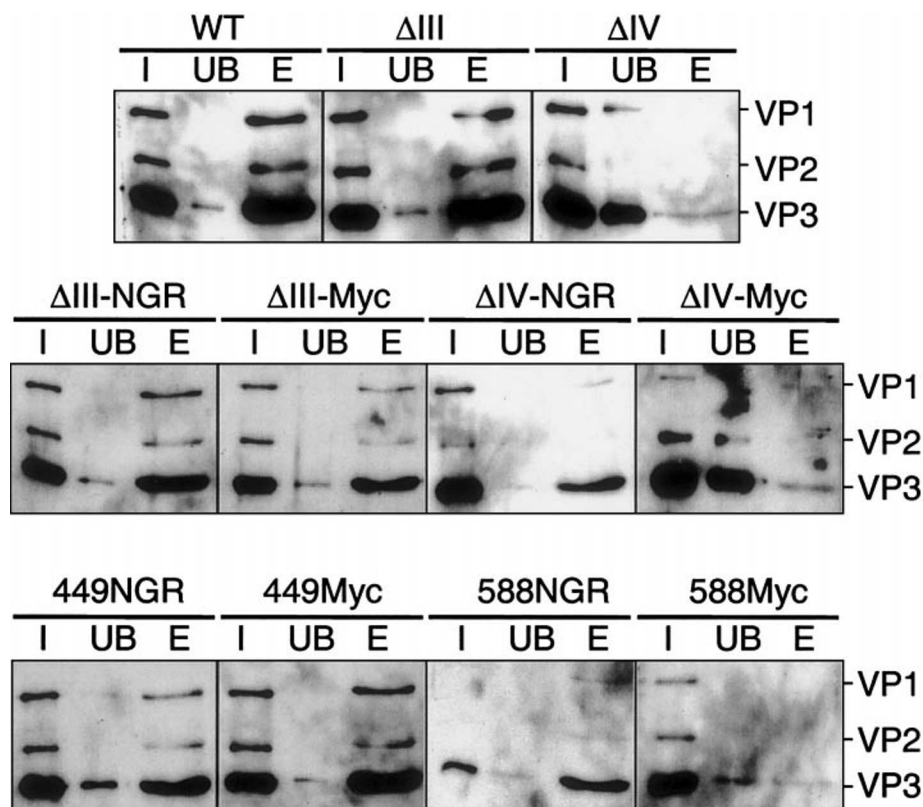


FIG. 5. Analysis of WT and mutant capsid virus binding to heparin. Iodixanol gradient-purified rAAV viruses were bound to heparin agarose for 1 h at 4°C. After extensive washing, bound virus was eluted with 1 M NaCl. The fractions were separated on SDS–8% acrylamide gels and analyzed by Western blotting using the B1 antibody. Shown are 5% of input virus (I), 5% of the unbound fraction (UB), and 20% of the eluted fraction (E). The positions of VP1, VP2, and VP3 are indicated.

Heparin Binding of AAV Capsids Containing Heterologous Peptide Sequences

One possible cause for the reduced infectivity of rAAV mutants containing foreign epitopes could be their inability to bind the viral cell surface receptors. A primary receptor for AAV-2 has been reported to be heparan sulfate proteoglycan (12). To test whether viruses with mutant capsids could bind heparin, we performed heparin batch binding experiments and detected the viruses by Western blotting using the B1 antibody (Fig. 5). Recombinant viruses purified by iodixanol gradient centrifugation were bound to heparin agarose for 1 h at 4°C. Following incubation of the viruses with heparin agarose, the unbound fraction was removed. After extensive washing of the heparin agarose, viruses were eluted in 1 M NaCl. As expected, viruses containing a wild-type capsid had a high affinity for the heparin agarose, and negligible amounts of virus were found in the unbound fraction. About 20% of the input virus was recovered in the elution from the beads. Most mutants had a binding and elution profile similar to that of the wild-type capsids. However, a deletion of 6 amino acids (GNRQAA) from Loop IV abolished binding to heparin. Interestingly, replacement of this sequence with the NGRAHA peptide sequence restored the ability of the mutant capsid to bind heparin

(Fig. 5). Viruses with the Myc epitope tag in the Loop IV region were unable to bind heparin, which suggests that this region is important for attachment to the primary receptor. This is also consistent with their poor transduction efficiency (Fig. 4).

Altered Tropism of rAAV Containing the Tumor-Targeting Peptides

To determine whether incorporation of targeting peptides could alter the tropism of rAAV we tested transduction on a number of cell lines (Fig. 6). For this purpose we employed two highly tumorigenic cell lines. Kaposi sarcoma (KS1767) cells are derived from Kaposi sarcoma lesions (38). The second cell line tested was an embryonal rhabdomyosarcoma cell line (RD). Both cell lines express high levels of CD13, the NGR receptor, as assessed by FACS analysis (RD and KS1767 were 57 and 99% positive for CD13 compared to 8 or 3% positive for 293T and HeLa cells). Viruses were first titrated on 293 cells and then equal transduction units of the different viruses were used to infect the other cells. An amount was chosen that resulted in 10% transduction of 293 cells as assessed by FACS analysis for GFP expression. Using these adjusted values, similar transduction efficiencies were seen for the viruses on HeLa cells (Figs. 6A and 6B). However, rAAV consisting

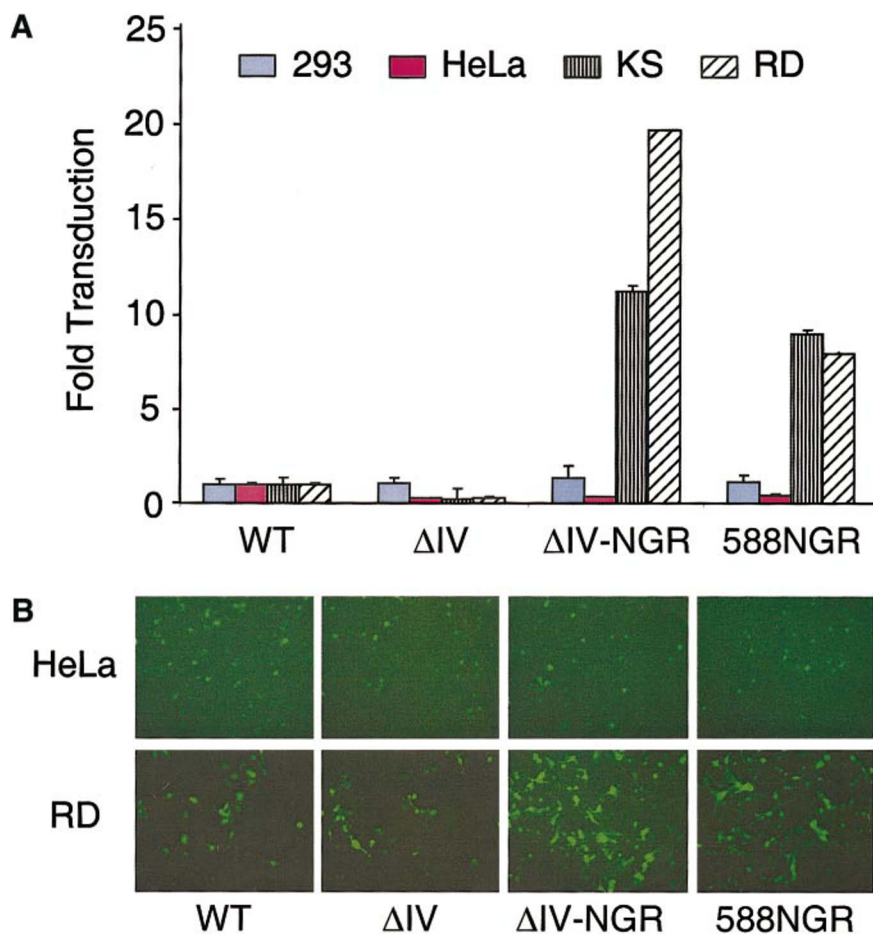


FIG. 6. Altered tropism of rAAV containing the NGRAHA sequence. Viruses were initially titrated for transduction on 293 cells by FACS analysis of GFP expression. An equal amount of transduction units (able to achieve 10% transduction of 293 cells) was used to infect 293, HeLa, KS1767, and RD cells. These correspond to 1×10^7 , 2×10^8 , 5×10^8 , and 4×10^8 genome-containing particles for WT, Δ IV, Δ IV-NGR, and 588NGR, respectively. Transduction was assessed at 24–72 h postinfection, by counting green cells under a fluorescence microscope or by FACS analysis. (A) Transduction efficiencies are shown relative to the wild-type capsid in the different cell lines. (B) Images of GFP expression captured by fluorescence microscopy. Transduction of HeLa cells was comparable for the different viruses but those containing NGR peptides showed preferential transduction of RD cells. There was a correlation between expression of CD13 (as measured by FACS analysis with the WM15 antibody) and altered tropism of NGR-containing viruses.

of wild-type capsids transduced the KS1767 and RD cell lines very poorly. In contrast, viruses containing the NGRAHA sequence at Loop IV, either as a replacement or as an insertion, were able to transduce these cell lines 10- to 20-fold better than wild type (Fig. 6A). This altered tropism was not observed for viruses with deletion of Loop IV or the Myc epitope at this site.

In the context of the phage coat protein or as a synthetic peptide, targeting was most efficient with cyclic peptides containing four cysteine residues (38). Based on the data from phage display libraries we included sequences containing the targeting NGR motif in the potentially cyclic (two cysteines) or double cyclic forms. Viruses containing the cyclic NGR sequences were less efficient than those with the linear peptide in transduction of 293 and HeLa cells but they also displayed enhanced tropism toward the tumorigenic, CD-13-positive cell lines RD and KS1767 (Table 1 and data not shown).

Several sequences have been isolated from phage display libraries and shown to home to different tissues *in vivo*. These include lung-, brain-, tumor-, and muscle-homing peptides (36, 55–57). We inserted a number of these targeting peptides into the 588 site, which we had defined as appropriate for accepting heterologous sequences (see Table 1). These included a GFE-containing peptide to target membrane dipeptidase expressed on lung vasculature (55), a muscle-homing peptide (56), and sequences identified in an *in vitro* phage display screen for NG2 proteoglycan binding sequences (57). Some of the viruses containing other targeting peptides were produced less efficiently and we were not able to observe altered tropism in the appropriate cell lines (Table 1). In general, we observed that smaller peptides were tolerated better than larger ones. Even at the same site we saw an effect of the sequence that was inserted, with linear peptides having fewer deleterious effects than sequences containing multiple cysteine residues.

TABLE 1

Properties of Recombinant AAV Viruses Containing Homing Peptides in Their Capsid Proteins

Virus ^a	Homing peptide ^b	Titer ^c (g.p./ml)	Transduction ^d (% of WT)	Cells ^e	Alt Trop ^f
588 GFE-4C	CGFECVRQCPERC	2.50×10^9	7.00	MBA-MBP ^g	—
588 NGR-2C	CNGRC	6.00×10^{10}	0.75	RD/KS1767	+
588 NGR-4C	CNGRCVSGCAGRC	4.30×10^9	0.75	RD/KS1767	+
588 L14	QAGTFALRGDNPQ	1.50×10^{10}	0.82	NA	ND
588 MH	ASSLNIA	7.70×10^{10}	1.12	NA	ND
588 NG2-1	TAASGVRSMH	1.00×10^{11}	1.3	B16F10NG2	—
588 NG2-2	LTLRWVGLMS	6.60×10^9	0.75	B16F10NG2	—

^a Homing peptides were introduced into the AAV capsid at amino acid 588 and recombinant viruses were produced in 293T cells using pXX6 as a helper to package a GFP expression cassette.

^b See text for details.

^c Viruses were purified by iodixanol gradient centrifugation and titered by real-time PCR. Titers are presented in genome-containing particles (g.p./ml).

^d Transduction was assessed in 293 cells by FACS analysis and is presented as a percentage of WT.

^e Cell lines used to assess targeting of an equal amount of transduction units as assessed on 293 cells. NA, not applicable.

^f Altered tropism was tested in the indicated cell lines. ND, not determined.

^g MDA-MB-435-MBP (59).

DISCUSSION

Homing peptides isolated by *in vivo* screening of phage display libraries provide novel tools for selective vascular targeting of therapies and are attractive for incorporation into viral vectors (36–38, 41, 58). It is unclear whether these peptides will be presented in the correct conformation on viral particles to enable targeting of modified vectors. We recently used targeting peptides to redirect adenoviral vectors to specific endothelial receptors using bispecific conjugates with antibodies recognizing adenovirus particles (59). Tumor-targeting peptides have also been successfully used to enhance the antitumor properties of doxorubicin and TNF (38, 40). In this study, we were able to generate modified AAV-2 capsids that contain targeting peptides, previously isolated by *in vivo* phage display. Peptides were incorporated as either replacements of native sequences or insertions. Modification of putative loops did not affect replication, assembly, and packaging of rAAV vectors. We show that the precise site of insertion and the choice of replacement of the original sequence can have an impact on the accessibility of the peptide at the capsid surface. We found that the transduction efficiency of rAAV-2 vectors bearing such peptides was severely compromised, but that in some cases we could demonstrate altered preference for transduction of tumor cells. This study represents the first attempt to target rAAV by genetic incorporation of tumor-targeting peptides previously isolated by phage display technologies. We were able to generate AAV viruses containing linear, cyclic, and double-cyclic versions of the NGR and these vectors showed altered tropism, with preferential transduction of cells that express the CD13 receptor.

Alignments of available sequences for all the parvovirus capsid proteins highlight large areas of sequence conser-

vation (29). Sequences that make up the β -barrel are the most conserved. Consistent with this are genetic studies in which mutations within these regions result in noninfectious viruses, many of which do not make intact capsids (34, 35, and M.G. and M.D.W., unpublished data). A comparison of our alignment to the previously published ones (29, 33) reveals some differences, especially in variable regions where sequence similarity is low and insertions are present. We have also extended the alignments presented in Fig. 1 by including additional parvoviral sequences (e.g., Kilhamrat, porcine, and simian), which enhance the confidence of the alignment we show (data not shown). When the three-dimensional structure of the AAV-2 capsid is solved, the validity of these hypothetical alignments will be assessed by superimposing the actual structures. We were able to make deletions within the putative Loops III and IV of AAV-2 without causing any detrimental effects on virus assembly or packaging. This is in contrast to previous studies with CPV, in which deletions in loops 1, 3, and 4 affected capsid assembly and morphology (60). It should be noted, however, that in the CPV study the deletions were larger (12–16 amino acids) and the assay for assembly was the formation of virus-like particles after infection of insect cells with recombinant baculoviruses expressing the Cap proteins. Despite our ability to modify these loop regions we encountered some residues that were far more sensitive to alterations. For example a single point mutation within Loop IV (Q584S) completely abrogated rAAV transduction (data not shown). The dramatic effect of deletions in Loops III or IV on transduction by rAAV vectors suggests that these two regions are indeed involved in the infectious pathway. This may be at the level of attachment to cellular receptors or some additional step during internalization, cytoplasmic trafficking, or nuclear entry of the virus particle.

Three cellular receptors have been implicated in AAV infection (HSPG, FGFR-1, and $\alpha_v\beta_5$ integrin) although direct involvement of these proteins has recently been called into question (61–63). We could confirm that putative Loop IV is required for binding to heparin, which is consistent with its attachment to the proposed HSPG primary receptor (12) and recent mapping of two heparin-binding clusters (34, 35). We have not yet investigated binding of these mutants to the putative secondary receptors. It is interesting to note that while deleting a part of Loop IV abolishes heparin binding, replacing it with the NGR targeting peptide could restore binding. Replacement of the same sequence in Loop IV with the Myc epitope was unable to rescue heparin binding. The NGR peptide is similar to the sequence that has been deleted, suggesting that replacement of capsid epitopes with residues resembling the original sequence in size and charge may be well tolerated.

In order for rAAV vectors with altered tropism to be viable for clinical applications it is important that the production, packaging, and transduction efficiencies of the modified viruses are not severely compromised. One previous attempt to target AAV capsids required transfection of the modified capsid construct together with wild-type virus and gave a very low yield of virus (32). We found that our modified viruses were similar to wild type in their ability to replicate and package a vector genome but in almost every case the transduction of the modified capsid was suboptimal. This has been a common problem for all attempts so far to retarget rAAV vectors (33, 35). Our data suggest that this is due to a combination of size, sequence, and insertion site. We have found that larger peptides tend to have more detrimental effects on the properties of the modified virus particle. While some peptides such as the NGR and L14 (33) have been tolerated for insertion in Loops III and IV, others such as the serpin ligand resulted in no capsid formation (35). We have been able to show altered tropism for vectors containing targeting peptides but in all cases this was at the expense of transduction efficiency, which would not be acceptable for clinical applications.

Successful retargeting of rAAV vectors is likely to come from a delicate combination of the type of peptide inserted and the choice of insertion site. A number of studies have now described multiple sites that can be used for peptide insertions (32–35). In this study we have focussed on a limited number of sites and inserted multiple different sequences in two approaches, replacements or insertions. Our data suggest that the best approach may be to scan the AAV sequence for putative surface-exposed areas that contain nonconserved protein sequences matching the sequence to be inserted and replace these regions with the targeting ligand. Perhaps this may be best achieved through a combinatorial library approach, whereby rAAV vectors with modified capsids are selected directly for a given target. Libraries could also be used to select for viruses that have inserted peptides but also maintain transduction levels similar to those of wild-type capsids. One potential problem with a small virus such as AAV is

that it is possible that receptor binding and other steps in the transduction process may be structurally linked, such as in CPV (64). Further studies of the pathways of AAV infection and rAAV transduction will reveal the role of different parts of the capsid in the infection entry process. The ability to restrict AAV-2 gene delivery to a specific organ or tissue will allow the use of smaller dosages of virus and will be important in limiting toxicity following systemic *in vivo* administration in a wide range of gene therapy applications.

ACKNOWLEDGMENTS

We thank David Chambers and Kelly Hardwicke for help with FACS analysis, Tom Hope for use of the fluorescence microscope and camera, Jude Samulski for plasmids, Sam Young for advice on heparin binding assays. We are grateful to Toni Cathomen, Travis Stracker, and Nik Somia for helpful discussions and for critically reading the manuscript. This work was supported by grants from the Department of Defense (DAMD 17-98-1-8041, to R.P. and M.D.W.) and the California Cancer Research Program (PF0071 to M.D.W.), an Innovation Grant from the Presidents' Club of the Salk Institute (M.D.W.), and the NIH. Martin Trepel was supported by the Deutsche Forschungsgemeinschaft (DFG) and by the Susan G. Komen Breast Cancer Foundation. Matthew D. Weitzman acknowledges gifts from the Mary H. Rumsey and Irving A. Hansen Foundations.

REFERENCES

- Monahan, P. E., and Samulski, R. J. (2000). AAV vectors: Is clinical success on the horizon? *Gene Ther.* 7: 24–30.
- Klein, R. L., Mandel, R. J., and Muzyczka, N. (2000). Adeno-associated virus vector-mediated gene transfer to somatic cells in the central nervous system. *Adv. Virus Res.* 55: 507–528.
- Xiao, X., Li, J., McCown, T. J., and Samulski, R. J. (1997). Gene transfer by adeno-associated virus vectors into the central nervous system. *Exp. Neurol.* 144: 113–124.
- Snyder, R. O., et al. (1997). Persistent and therapeutic concentrations of human factor IX in mice after hepatic gene transfer of recombinant AAV vectors. *Nat. Genet.* 16: 270–276.
- Flotte, T. R., et al. (1993). Stable *in vivo* expression of the cystic fibrosis transmembrane conductance regulator with an adeno-associated virus vector. *Proc. Natl. Acad. Sci. USA* 90: 10613–10617.
- Fisher, K. J., et al. (1997). Recombinant adeno-associated virus for muscle directed gene therapy. *Nat. Med.* 3: 306–312.
- Halbert, C. L., Standaert, T. A., Aitken, M. L., Alexander, I. E., Russell, D. W., and Miller, A. D. (1997). Transduction by adeno-associated virus vectors in the rabbit airway: Efficiency, persistence, and readministration. *J. Virol.* 71: 5932–5941.
- Ponnazhagan, S., et al. (1997). Adeno-associated virus type 2-mediated transduction in primary human bone marrow-derived CD34⁺ hematopoietic progenitor cells: Donor variation and correlation of transgene expression with cellular differentiation. *J. Virol.* 71: 8262–8267.
- Bartlett, J. S., Kleinschmidt, J., Boucher, R. C., and Samulski, R. J. (1999). Targeted adeno-associated virus vector transduction of nonpermissive cells mediated by a bispecific F(ab')₂ antibody. *Nat. Biotechnol.* 17: 181–186.
- Mizukami, H., Young, N. S., and Brown, K. E. (1996). Adeno-associated virus type 2 binds to a 150-kilodalton cell membrane glycoprotein. *Virology* 217: 124–130.
- Ponnazhagan, S., et al. (1996). Differential expression in human cells from the p6 promoter of human parvovirus B19 following plasmid transfection and recombinant adeno-associated virus 2 (AAV) infection: Human megakaryocytic leukaemia cells are non-permissive for AAV infection. *J. Gen. Virol.* 77: 1111–1122.
- Summerford, C., and Samulski, R. J. (1998). Membrane-associated heparan sulfate proteoglycan is a receptor for adeno-associated virus type 2 virions. *J. Virol.* 72: 1438–1445.
- Qing, K., Mah, C., Hansen, J., Zhou, S., Dwarki, V., and Srivastava, A. (1999). Human fibroblast growth factor receptor 1 is a co-receptor for infection by adeno-associated virus 2. *Nat. Med.* 5: 71–77.
- Summerford, C., Bartlett, J. S., and Samulski, R. J. (1999). AlphaVbeta5 integrin: A co-receptor for adeno-associated virus type 2 infection. *Nat. Med.* 5: 78–82.
- Sanlioglu, S., Benson, P. K., Yang, J., Atkinson, E. M., Reynolds, T., and Engelhardt, J. F. (2000). Endocytosis and nuclear trafficking of adeno-associated virus type 2 are controlled by rac1 and phosphatidylinositol-3 kinase activation. *J. Virol.* 74: 9184–9196.
- Duan, D., Li, Q., Kao, A. W., Yue, Y., Pessin, J. E., and Engelhardt, J. F. (1999). Dynamin is required for recombinant adeno-associated virus type 2 infection. *J. Virol.* 73: 10371–10376.
- Bartlett, J. S., Wilcher, R., and Samulski, R. J. (2000). Infectious entry pathway of adeno-associated virus and adeno-associated virus vectors. *J. Virol.* 74: 2777–2785.
- Weitzman, M. D., Fisher, K. J., and Wilson, J. M. (1996). Recruitment of wild-type and recombinant adeno-associated virus into adenovirus replication centers. *J. Virol.* 70: 1845–1854.
- Hansen, J., Qing, K., Kwon, H. J., Mah, C., and Srivastava, A. (2000). Impaired

intracellular trafficking of adeno-associated virus type 2 vectors limits efficient transduction of murine fibroblasts. *J. Virol.* **74**: 992–996.

²⁰ Berns, K. I. (1974). Molecular biology of the adeno-associated viruses. *Curr. Top. Microbiol. Immunol.* **65**: 1–20.

²¹ Laughlin, C. A., Tratschin, J. D., Coon, H., and Carter, B. J. (1983). Cloning of infectious adeno-associated virus genomes in bacterial plasmids. *Gene* **23**: 65–73.

²² Samulski, R. J., Berns, K. I., Tan, M., and Muzyczka, N. (1982). Cloning of adeno-associated virus into pBR322: Rescue of intact virus from the recombinant plasmid in human cells. *Proc. Natl. Acad. Sci. USA* **79**: 2077–2081.

²³ Berns, K. I. (1996). Parvoviridae: The viruses and their replication. In *Virology* (D. M. Knipe, B. N. Fields, P. M. Howley, Eds.), pp. 2173–2197. Lippincott-Raven, Philadelphia.

²⁴ Becerra, S. P., Kocot, F., Fabisch, P., and Rose, J. A. (1988). Synthesis of adeno-associated virus structural proteins requires both alternative mRNA splicing and alternative initiations from a single transcript. *J. Virol.* **62**: 2745–2754.

²⁵ Tsao, J., et al. (1991). The three-dimensional structure of canine parvovirus and its functional implications. *Science* **251**: 1456–1464.

²⁶ Agbandje, M., McKenna, R., Rossmann, M. G., Strassheim, M. L., and Parrish, C. R. (1993). Structure determination of feline panleukopenia virus empty particles. *Proteins* **16**: 155–171.

²⁷ Agbandje-McKenna, M., Llamas-Saiz, A. L., Wang, F., Tattersall, P., and Rossmann, M. G. (1998). Functional implications of the structure of the murine parvovirus, minute virus of mice. *Structure* **6**: 1369–1381.

²⁸ Agbandje, M., Kajigaya, S., McKenna, R., Young, N. S., and Rossmann, M. G. (1994). The structure of human parvovirus B19 at 8 Å resolution. *Virology* **203**: 106–115.

²⁹ Chapman, M. S., and Rossmann, M. G. (1993). Structure, sequence, and function correlations among parvoviruses. *Virology* **194**: 491–508.

³⁰ Wobus, C. E., Hugle-Dorr, B., Girod, A., Petersen, G., Hallek, M., and Kleinschmidt, J. A. (2000). Monoclonal antibodies against the adeno-associated virus type 2 (AAV-2) capsid: Epitope mapping and identification of capsid domains involved in AAV-2-cell interaction and neutralization of AAV-2 infection. *J. Virol.* **74**: 9281–9293.

³¹ Moskalenko, M., et al. (2000). Epitope mapping of human anti-adeno-associated virus type 2 neutralizing antibodies: Implications for gene therapy and virus structure. *J. Virol.* **74**: 1761–1766.

^{31a} Rabinowitz, J. E., and Samulski, R. J. (2000). Building a better vector: The manipulations of AAV virions. *Virology* **278**: 301–308.

³² Yang, Q., et al. (1998). Development of novel cell surface CD34-targeted recombinant adeno-associated virus vectors for gene therapy. *Hum. Gene Ther.* **9**: 1929–1937.

³³ Girod, A., et al. (1999). Genetic capsid modifications allow efficient re-targeting of adeno-associated virus type 2. *Nat. Med.* **5**: 1438.

³⁴ Rabinowitz, J. E., Xiao, W., and Samulski, R. J. (1999). Insertional mutagenesis of AAV2 capsid and the production of recombinant virus. *Virology* **265**: 274–285.

³⁵ Wu, P., et al. (2000). Mutational analysis of the adeno-associated virus type 2 (AAV2) capsid gene and construction of AAV2 vectors with altered tropism. *J. Virol.* **74**: 8635–8647.

³⁶ Pasqualini, R., and Ruoslahti, E. (1996). Organ targeting in vivo using phage display peptide libraries. *Nature* **380**: 364–366.

³⁷ Rajotte, D., Arap, W., Hagedorn, M., Koivunen, E., Pasqualini, R., and Ruoslahti, E. (1998). Molecular heterogeneity of the vascular endothelium revealed by in vivo phage display. *J. Clin. Invest.* **102**: 430–437.

³⁸ Arap, W., Pasqualini, R., and Ruoslahti, E. (1998). Cancer treatment by targeted drug delivery to tumor vasculature in a mouse model. *Science* **279**: 377–380.

³⁹ Pasqualini, R., et al. (2000). Aminopeptidase N is a receptor for tumor-homing peptides and a target for inhibiting angiogenesis. *Cancer Res.* **60**: 722–727.

⁴⁰ Curnis, F., Sacchi, A., Borgna, L., Magni, F., Gasparri, A., and Corti, A. (2000). Enhancement of tumor necrosis factor alpha antitumor immunotherapeutic properties by targeted delivery to aminopeptidase N (CD13). *Nat. Biotechnol.* **18**: 1185–1190.

⁴¹ Koivunen, E., et al. (1999). Tumor targeting with a selective gelatinase inhibitor. *Nat. Biotechnol.* **17**: 768–774.

⁴² Li, J., Samulski, R. J., and Xiao, X. (1997). Role for highly regulated rep gene expression in adeno-associated virus vector production. *J. Virol.* **71**: 5236–5243.

⁴³ Xiao, X., Li, J., and Samulski, R. J. (1998). Production of high-titer recombinant adeno-associated virus vectors in the absence of helper adenovirus. *J. Virol.* **72**: 2224–2232.

⁴⁴ Zolotukhin, S., et al. (1999). Recombinant adeno-associated virus purification using novel methods improves infectious titer and yield. *Gene Ther.* **6**: 973–985.

⁴⁵ Clark, K. R., Liu, X., McGrath, J. P., and Johnson, P. R. (1999). Highly purified recombinant adeno-associated virus vectors are biologically active and free of detectable helper and wild-type viruses. *Hum. Gene Ther.* **10**: 1031–1039.

⁴⁶ Muramatsu, S., Mizukami, H., Young, N. S., and Brown, K. E. (1996). Nucleotide sequencing and generation of an infectious clone of adeno-associated virus 3. *Virology* **221**: 208–217.

⁴⁷ Bantel-Schaal, U., Delius, H., Schmidt, R., and zur Hausen, H. (1999). Human adeno-associated virus type 5 is only distantly related to other known primate helper-dependent parvoviruses. *J. Virol.* **73**: 939–947.

⁴⁸ Xiao, W., Chirmule, N., Berta, S. C., McCullough, B., Gao, G., and Wilson, J. M. (1999). Gene therapy vectors based on adeno-associated virus type 1. *J. Virol.* **73**: 3994–4003.

⁴⁹ Chiorini, J. A., Kim, F., Yang, L., and Kotin, R. M. (1999). Cloning and characterization of adeno-associated virus type 5. *J. Virol.* **73**: 1309–1319.

⁵⁰ Rutledge, E. A., Halbert, C. L., and Russell, D. W. (1998). Infectious clones and vectors derived from adeno-associated virus (AAV) serotypes other than AAV type 2. *J. Virol.* **72**: 309–319.

⁵¹ Langeveld, J. P., et al. (1993). B-cell epitopes of canine parvovirus: Distribution on the primary structure and exposure on the viral surface. *J. Virol.* **67**: 765–772.

⁵² Strassheim, M. L., Gruenberg, A., Veijalainen, P., Sgro, J. Y., and Parrish, C. R. (1994). Two dominant neutralizing antigenic determinants of canine parvovirus are found on the threefold spike of the virus capsid. *Virology* **198**: 175–184.

⁵³ Yoshimoto, K., et al. (1991). A second neutralizing epitope of B19 parvovirus implicates the spike region in the immune response. *J. Virol.* **65**: 7056–7060.

⁵⁴ Fisher, K. J., Gao, G.-P., Weitzman, M. D., DeMatteo, R., Burda, J. F., and Wilson, J. M. (1996). Transduction with recombinant adeno-associated virus for gene therapy is limited by leading strand synthesis. *J. Virol.* **70**: 520–532.

⁵⁵ Rajotte, D., and Ruoslahti, E. (1999). Membrane dipeptidase is the receptor for a lung-targeting peptide identified by in vivo phage display. *J. Biol. Chem.* **274**: 11593–11598.

⁵⁶ Samoylova, T. I., and Smith, B. F. (1999). Elucidation of muscle-binding peptides by phage display screening. *Muscle Nerve* **22**: 460–466.

⁵⁷ Burg, M. A., Pasqualini, R., Arap, W., Ruoslahti, E., and Stallcup, W. B. (1999). NG2 proteoglycan-binding peptides target tumor neovasculature. *Cancer Res.* **59**: 2869–2874.

⁵⁸ Arap, W., Pasqualini, R., and Ruoslahti, E. (1998). Chemotherapy targeted to tumor vasculature. *Curr. Opin. Oncol.* **10**: 560–565.

⁵⁹ Trepel, M., Grifman, M., Weitzman, M. D., and Pasqualini, R. (2000). Molecular adaptors for vascular-targeted adenoviral gene delivery. *Hum. Gene Ther.* **11**: 1971–1981.

⁶⁰ Hurtado, A., Rueda, P., Nowicky, J., Sarraesca, J., and Casal, J. I. (1996). Identification of domains in canine parvovirus VP2 essential for the assembly of virus-like particles. *J. Virol.* **70**: 5422–5429.

⁶¹ Qiu, J., Handa, A., Kirby, M., and Brown, K. E. (2000). The interaction of heparin sulfate and adeno-associated virus 2. *Virology* **269**: 137–147.

⁶² Qiu, J., and Brown, K. E. (1999). Integrin α 5 β 1 is not involved in adeno-associated virus type 2 (AAV2) infection. *Virology* **264**: 436–440.

⁶³ Qiu, J., Mizukami, H., and Brown, K. E. (1999). Adeno-associated virus 2 co-receptors? *Nat. Med.* **5**: 467–468.

⁶⁴ Simpson, A. A., Chandrasekar, V., Hebert, B., Sullivan, G. M., Rossmann, M. G., and Parrish, C. R. (2000). Host range and variability of calcium binding by surface loops in the capsids of canine and feline parvoviruses. *J. Mol. Biol.* **300**: 597–610.